

Comparison of Species and Cell-Type Differences in Fraction Unbound of Liver Tissues, Hepatocytes, and Cell Lines[§]

Keith Riccardi, Sangwoo Ryu, Jian Lin, Phillip Yates, David Tess, Rui Li, Dhirender Singh,¹
Brian R. Holder,² Brendon Kapinos, George Chang, and Li Di

Pharmacokinetics, Dynamics and Metabolism, Pfizer Inc., Groton, Connecticut (K.R., S.R., J.L., D.S., B.R.H., B.K., G.C., L.D.); and Early Clinical Development (P.Y.), and Pharmacokinetics, Dynamics and Metabolism (D.T., R.L.), Pfizer Inc., Cambridge, Massachusetts

Received October 23, 2017; accepted January 24, 2018

ABSTRACT

Fraction unbound (f_u) of liver tissue, hepatocytes, and other cell types is an essential parameter used to estimate unbound liver drug concentration and intracellular free drug concentration. $f_{u,liver}$ and $f_{u,cell}$ are frequently measured in multiple species and cell types in drug discovery and development for various applications. A comparison study of 12 matrices for $f_{u,liver}$ and $f_{u,cell}$ of hepatocytes in five different species (mouse, rat, dog, monkey, and human), as well as $f_{u,cell}$ of Huh7 and human embryonic kidney 293 cell lines, was conducted for 22 structurally diverse compounds with the equilibrium dialysis method. Using an average bioequivalence approach, our results show that the

average difference in binding to liver tissue, hepatocytes, or different cell types was within 2-fold of that of the rat $f_{u,liver}$. Therefore, we recommend using rat $f_{u,liver}$ as a surrogate for liver binding in other species and cell types in drug discovery. This strategy offers the potential to simplify binding studies and reduce cost, thereby enabling a more effective and practical determination of f_u for liver tissues, hepatocytes, and other cell types. In addition, f_u under hepatocyte stability incubation conditions should not be confused with $f_{u,cell}$, as one is a diluted f_u and the other is an undiluted f_u . Cell density also plays a critical role in the accurate measurement of $f_{u,cell}$.

Introduction

For disease targets residing in the tissues (e.g., liver, brain, or muscle), free drug concentrations in tissues are critical for in vivo efficacy and for the development of pharmacokinetics/pharmacodynamics relationships (Smith et al., 2010). The fraction unbound (f_u) of tissues is essential for the determination of in vivo free drug concentrations in the tissues, as total tissue drug concentrations are usually measured in vivo, and free drug concentration is then calculated by multiplying total drug concentration with f_u (i.e., free drug concentration = total drug concentration $\times f_u$). The liver is an important organ for a number of therapeutic targets, such as diabetes, dyslipidemia, obesity, and non-alcoholic steatohepatitis. Recent strategies for liver targeting by utilizing liver-specific uptake transporters [e.g., organic anion-transporting polypeptide (OATP) 1B1 and OATP1B3] have shown promise in enhancing efficacy in the liver and minimizing side effects in peripheral tissues (Oballa et al., 2011; Pfefferkorn, 2013; Tu et al., 2013). Even for compounds that are not liver targeting by design, their clearance and disposition can still be mediated by transporters (Li et al., 2014). For these cases, liver-free drug concentration might not be the same as plasma-free drug concentration due to the impact of transporters

(Pfefferkorn et al., 2012). Therefore, an accurate determination of f_u of liver tissue ($f_{u,liver}$) is important to estimate free liver drug concentration. With increasing knowledge of the effects of hepatobiliary influx and efflux transporters on drug disposition, our ability to predict free liver drug concentration is critical for assessing efficacy, therapeutic index, the potential for drug-drug interactions, and toxicity. For in vitro cell-based assays, such as metabolic stability, induction, inhibition, and pharmacological assays, f_u measurements of hepatocytes or other cell types [f_u of cells ($f_{u,cell}$)] allows for the determination of intracellular free drug concentration (Mateus et al., 2013; Riccardi et al., 2016, 2017). Intracellular free drug concentration, rather than nominal concentration, is most relevant for compounds with intracellular accumulation or exclusion to develop in vitro-in vivo correlations for human translation and to understand the in vitro absorption, distribution, metabolism, excretion, and toxicity and pharmacology endpoints (Riccardi et al., 2016, 2017; Mateus et al., 2017; Riede et al., 2017; Sun et al., 2017). Using intracellular free drug concentration, the unbound partition coefficient (K_{puu}) can be determined and used to derive intrinsic activity for in vitro cell-based assays (e.g., $CL_{int} = CL_{int}'/K_{puu}$, $EC_{50} = EC_{50}' \times K_{puu}$, $IC_{50} = IC_{50}' \times K_{puu}$, where CL_{int} is intrinsic clearance, CL_{int}' is apparent intrinsic clearance, EC_{50}' is apparent EC_{50} , and IC_{50}' is apparent IC_{50}).

Binding to liver tissues and cells (e.g., hepatocytes, Huh7, and HEK-293) is routinely measured in various species and cell types matching the corresponding in vivo and in vitro studies, partly because species and cell type-dependent binding is mostly unexplored. Recent studies of $f_{u,cell}$ in HEK-293 cells have shown good correlation between human and

¹Current affiliation: Navinta LLC, Ewing, New Jersey.

²Current affiliation: PerkinElmer, Shelton, Connecticut.

<https://doi.org/10.1124/dmd.117.079152>.

[§]This article has supplemental material available at dmd.aspetjournals.org.

ABBREVIATIONS: ACN, acetonitrile; CI, confidence interval; D, dilution factor; DMEM, Dulbecco's modified eagles medium; f_u , fraction unbound; $f_{u,cell}$, fraction unbound of cells; $f_{u,d}$, diluted fraction unbound; $f_{u,inc}$, fraction unbound under incubation conditions; $f_{u,liver}$, fraction unbound of liver tissues; HEK-293, human embryonic kidney 293; HPLC, high-performance liquid chromatography; Huh7, human hepatocyte-derived carcinoma cell line; IS, internal standard; K_{puu} , unbound partition coefficient; LC-MS/MS liquid chromatography coupled with tandem mass spectrometry; OATP, organic anion-transporting polypeptide; PBS, phosphate-buffered saline; TOST, two one-sided test.

TABLE 1
Cell diameters and dilution factors of cell homogenates

Cells	Diameter \pm S.D.	Cell Volume	D at 50 Million Cells/ml
	μm	$\mu\text{l}/\text{million cells}$	
Mouse hepatocyte	19.7 ± 1.5	4.00	5.00
Rat hepatocyte	19.1 ± 0.74	3.65	5.48
Dog hepatocyte	15.8 ± 0.93	2.07	9.69
Monkey hepatocyte	15.0 ± 0.64	1.77	11.3
Human hepatocyte	17.3 ± 1.5	2.71	7.38
Huh7 cells	14.1 ± 0.33	1.47	13.6
HEK-293 cells	14.3 ± 0.83	1.53	13.1

rat hepatocyte binding after a 4-fold to 6-fold correction of dilution factor (D), defined as the total suspension volume divided by cell volume (Mateus et al., 2013). This suggested that binding might be independent of cell type and species with correction factors for the concentrations of the binding components in cell and tissue homogenates. Furthermore, it has also been reported that binding to phospholipids is mostly responsible for liver microsomal binding (Margolis and Obach, 2003), which suggests that binding to hepatocytes is likely to be species and/or cell type independent. Plasma protein binding has been shown to be species dependent due to specific binding to certain plasma proteins (Kratochwil et al., 2004; Di and Kerns, 2016). In contrast, binding to brain tissue has been reported to be independent of species as it is mostly driven by nonspecific binding to phospholipids in brain tissue (Summerfield et al., 2008; Read and Braggio, 2010; Di et al., 2011). For exploration, it would be very useful to determine whether binding to liver tissues, hepatocytes, and various cells that are commonly used in drug discovery are species and cell type independent. Herein, we discuss the evaluation of $f_{u,\text{liver}}$ and $f_{u,\text{cell}}$ in multiple species for 22 structurally diverse compounds using the equilibrium dialysis method. Overall, these efforts will help to determine whether liver binding from a single species can be used to represent binding for all common species and cell types. The anticipated outcome of this study is geared toward the simplification of liver tissue and cell-binding studies to inform free tissue and intracellular free drug concentrations with the added benefit of reducing costs in drug discovery.

Materials and Methods

Materials. Liver tissue of CD-1 mouse, cynomolgus monkey, and hepatocytes from all species were purchased from BioreclamationIVT, LLC (Hicksville, NY). Human liver tissue was obtained from Analytical Biologic Services Inc. (Wilmington, DE). Wistar Han rat liver and beagle dog liver were obtained in-house at Pfizer Research and Development (Groton, CT). All tissue samples were collected from animals in accordance with regulations and established guidelines including review and approval by an Institutional Animal Care and Use Committee. HEK-293 and Huh7 cells were purchased from American Type Culture Collection (Manassas, VA). Test compounds were obtained from Pfizer Global Material Management or purchased from Sigma-Aldrich (St. Louis, MO). Dulbecco's modified Eagles medium (DMEM), penicillin streptomycin, sodium pyruvate, and trypsin-EDTA were obtained from Life Technologies (Carlsbad, CA). Fetal bovine serum and all HPLC solvents were purchased from Sigma-Aldrich, and HEPES was purchased from Lonza (Walkersville, MD). The 96-well equilibrium dialysis (HTD 96) device and cellulose membranes with molecular mass cutoff of 12–14 kDa were obtained from HTDialysis, LLC (Gales Ferry, CT). Microtiter 96-deep well plates with a 1.2 ml capacity were obtained from Thermo Fisher Scientific (Waltham, MA), and T175 flasks were obtained from Corning Inc. (Corning, NY).

Cell Culture for HEK-293 and Huh7 Cell Lines. HEK-293 and Huh7 cells were cultured using DMEM, supplemented with 10% fetal bovine serum, 25 mM HEPES, 1% penicillin streptomycin, and 1% sodium pyruvate. Cells were trypsinized using trypsin-EDTA and passaged either at 1:10 for HEK-293 cells or

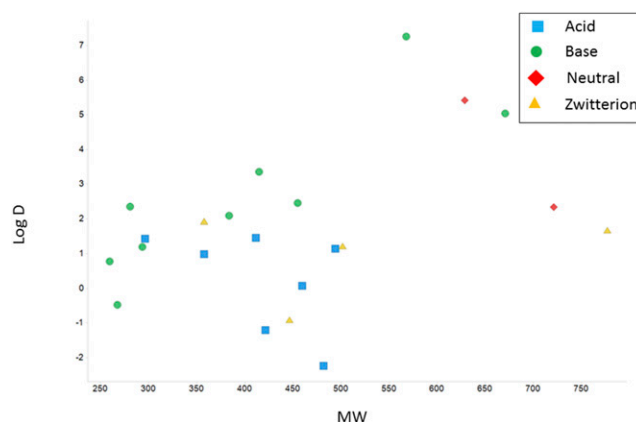


Fig. 1. Physicochemical properties of the 22 test compounds. MW, molecular weight.

1:5 for Huh7 cells into T175 flasks containing 25 ml of DMEM media with supplements. Cells were incubated at 37°C/5% CO₂/75% relative humidity for 4 days to reach confluence. Cell passages ranging from 10 to 25 were used for binding studies.

Preparation of Liver Tissue, Hepatocytes, and Cell Homogenates. Liver tissue samples (nonperfused) were rinsed with water to wash away the residual blood after harvest and subsequently were dried with paper towel. The procedure has been effective in removing blood from the liver tissue. Tissue samples were frozen at -20°C before use. Dulbecco's phosphate-buffered saline (PBS, without Ca^{2+} or Mg^{2+} ; VWR, Bridgeport, NJ) in four times the liver tissue weight (v/w) was added to the preweighted liver tissues ($D = 5$). The liver tissues were homogenized in PBS using a TH tissue homogenizer (Omni International, Kennesaw, GA) with a 7×110 mm tip at high speed for 30-second pulses. The liver homogenate suspensions were aliquoted into small portions and frozen at -20°C for future use. The liver suspensions were homogenized again before each dialysis experiment to ensure the formation of a homogeneous suspension. For hepatocytes and cells, a cell density of 40–60 million cells/ml suspension was prepared in PBS and homogenized as discussed above. Diameters of the cells were measured using Vi-CELL (Beckman Coulter, Danvers, MA) at an average cell density of 2.5×10^6 cells/ml. Cell volumes were calculated using cell diameters assuming a spherical shape. D was calculated by dividing the total cell suspension volume by the cell volume (Table 1).

Equilibrium Dialysis. The dialysis membranes were prepared prior to experimental setup. The cellulose membranes (molecular weight cutoff, 12–14 kDa) were immersed in deionized water for 15 minutes, followed by 15 minutes in 30% EtOH/deionized water, then at least 15 minutes or overnight in PBS. The equilibrium dialysis device (HTD 96) was assembled according to manufacturer instructions (<http://www.htdialysis.com/>). Dimethylsulfoxide stock solutions of test compounds were prepared at 200 μM , added in a 1:100 ratio to liver or cell homogenates, and mixed thoroughly with an eight-channel pipettor (Eppendorf; VWR, Radnor, PA). The final compound concentration for the equilibrium dialysis experiments was 2 μM , containing 1% dimethylsulfoxide. A 150 μl aliquot of tissue or cell homogenates spiked with 2 μM test compound was added to one side of the dialysis chamber (donor), and 150 μl of PBS was added to the other side of the dialysis membrane (receiver). Each compound was assessed in quadruplicate. Before and after incubation, an aliquot of 15 μl of homogenates spiked with 2 μM compounds was added to a 96-deep well plate containing 45 μl of PBS and mixed well. Two hundred microliters of cold acetonitrile (ACN) with mass spectrometry internal standard [IS (a cocktail of 0.5 ng/ml tolbutamide and 5 ng/ml terfenadine)] was added to precipitate the proteins/tissues. These samples were used as time zero to assess recovery of the assay and compound stability during incubation. The HTD 96 equilibrium dialysis device was covered with a Breathe Easy gas-permeable membrane (Sigma-Aldrich), placed on an orbital shaker (VWR) at 200 rpm, and incubated for 6 hours in a humidified (75% relative humidity) incubator at 37°C with 5% CO₂/95% air. At the end of the incubation, 15 μl of homogenate samples from the donor wells were taken and added to a 96-deep well plate containing 45 μl of PBS and mixed well. Aliquots of 45 μl dialyzed PBS were taken from the receiver wells and added to 15 μl of blank homogenates to achieve matrix-match and mixed

TABLE 2
 f_u for liver tissues, hepatocytes, and cells for several species and cell types

#	Compound	Liver				Hepatocytes				Human	Huh7	HEK-293
		Mouse	Rat	Dog	Monkey	Human	Mouse	Rat	Dog	Monkey		
1	Cerivastatin	0.0172 ± 0.0005	0.0109 ± 0.0012	0.0195 ± 0.0032	0.0212 ± 0.0013	0.0214 ± 0.0017	0.0101 ± 0.0015	0.0109 ± 0.0009	0.0112 ± 0.0005	0.0352 ± 0.0021	0.0199 ± 0.0043	0.0232 ± 0.0021
2	Diclofenac	0.0406 ± 0.0038	0.0624 ± 0.0040	0.0572 ± 0.0033	0.0496 ± 0.0039	0.0598 ± 0.0061	0.0223 ± 0.0037	0.0421 ± 0.0151	0.0412 ± 0.0029	0.119 ± 0.0173	0.0617 ± 0.0127	0.0392 ± 0.0021
3	Diltiazem	0.0252 ± 0.0015	0.0301 ± 0.0058	0.0339 ± 0.0035	0.0187 ± 0.0010	0.0287 ± 0.0021	0.0399 ± 0.0059	0.0327 ± 0.0083	0.0353 ± 0.0006	0.0349 ± 0.0024	0.0318 ± 0.0044	0.0196 ± 0.0012
4	Fexofenadine	0.1345 ± 0.0129	0.0792 ± 0.0022	0.0631 ± 0.0057	0.1345 ± 0.0129	0.1049 ± 0.0058	0.0743 ± 0.0061	0.0969 ± 0.0248	0.1313 ± 0.0206	0.122 ± 0.0189	0.0932 ± 0.0245	0.0711 ± 0.0054
5	Fluvastatin	0.0125 ± 0.0010	0.0157 ± 0.0005	0.0150 ± 0.0022	0.0322 ± 0.0051	0.0237 ± 0.0017	0.0184 ± 0.0021	0.0248 ± 0.0078	0.0076 ± 0.0008	0.0086 ± 0.0007	0.0290 ± 0.0014	0.0136 ± 0.0025
6	Glyburide	0.0396 ± 0.0023	0.0466 ± 0.0073	0.0351 ± 0.0108	0.0309 ± 0.0026	0.0490 ± 0.0020	0.0162 ± 0.0013	0.0364 ± 0.0153	0.0079 ± 0.0057	0.0047 ± 0.0047	0.0308 ± 0.0042	0.0614 ± 0.0069
7	Imipramine	0.0512 ± 0.0019	0.0396 ± 0.0036	0.0454 ± 0.0063	0.0305 ± 0.0006	0.0258 ± 0.0037	0.0297 ± 0.0021	0.0445 ± 0.0106	0.0162 ± 0.0013	0.0512 ± 0.0065	0.0579 ± 0.0093	0.0247 ± 0.0043
8	Indomethacin	0.0480 ± 0.0060	0.0528 ± 0.0099	0.0390 ± 0.0074	0.0419 ± 0.0026	0.0610 ± 0.0062	0.0272 ± 0.0022	0.0311 ± 0.0073	0.0366 ± 0.0034	0.0563 ± 0.0113	0.0521 ± 0.0136	0.0543 ± 0.0052
9	Levothroxine	0.0023 ± 0.0004	0.0015 ± 0.0003	0.0011 ± 0.0002	0.0022 ± 0.0001	0.0025 ± 0.0004	0.0009 ± 0.0001	0.0013 ± 0.0001	0.0021 ± 0.0002	0.0029 ± 0.0003	0.0025 ± 0.0003	0.0011 ± 0.0001
10	Lopinavir	0.0027 ± 0.0004	0.0030 ± 0.0006	0.0011 ± 0.0002	0.0021 ± 0.0002	0.0022 ± 0.0002	0.0031 ± 0.0005	0.0011 ± 0.0003	0.0019 ± 0.0001	0.0023 ± 0.0004	0.0036 ± 0.0005	0.0046 ± 0.0004
11	Metoprolol	0.364 ± 0.038	0.1953 ± 0.0359	0.1172 ± 0.0096	0.273 ± 0.0153	0.149 ± 0.0173	0.267 ± 0.0618	0.205 ± 0.0377	0.169 ± 0.0427	0.133 ± 0.040	0.195 ± 0.0289	0.309 ± 0.0954
12	Nelfinavir	0.0009 ± 0.0001	0.0008 ± 0.0001	0.0009 ± 0.0002	0.0018 ± 0.0001	0.0005 ± 0.0001	0.0007 ± 0.0001	0.0008 ± 0.0001	0.0014 ± 0.0002	0.0015 ± 0.0001	0.0017 ± 0.0001	0.0015 ± 0.0002
13	Olmesartan	0.411 ± 0.081	0.2371 ± 0.0618	0.2230 ± 0.0503	0.506 ± 0.0208	0.211 ± 0.033	0.139 ± 0.0173	0.295 ± 0.0594	0.142 ± 0.0171	0.235 ± 0.038	0.136 ± 0.041	0.1333 ± 0.0058
14	Ondansetron	0.0863 ± 0.0094	0.0959 ± 0.0100	0.0991 ± 0.0177	0.0812 ± 0.0163	0.0689 ± 0.0044	0.0449 ± 0.0035	0.0974 ± 0.0093	0.0647 ± 0.0118	0.126 ± 0.024	0.0818 ± 0.0104	0.0921 ± 0.0303
15	Pitavastatin	0.0174 ± 0.0024	0.0283 ± 0.0042	0.0358 ± 0.0042	0.0230 ± 0.0008	0.0405 ± 0.0057	0.0317 ± 0.0012	0.0192 ± 0.0031	0.0203 ± 0.0031	0.0169 ± 0.0018	0.0466 ± 0.0039	0.0206 ± 0.0012
16	Prazosin	0.0236 ± 0.0012	0.100 ± 0.000	0.0227 ± 0.0010	0.0591 ± 0.0118	0.0529 ± 0.0067	0.0534 ± 0.0093	0.109 ± 0.0226	0.0697 ± 0.0034	0.0626 ± 0.0050	0.0318 ± 0.0042	0.0569 ± 0.0039
17	Propranolol	0.0332 ± 0.0040	0.0183 ± 0.0045	0.0273 ± 0.0021	0.0304 ± 0.0025	0.0087 ± 0.0005	0.0127 ± 0.0013	0.0226 ± 0.0026	0.0197 ± 0.0022	0.0297 ± 0.0074	0.0119 ± 0.0014	0.0390 ± 0.0049
18	Ritonavir	0.0057 ± 0.0008	0.0026 ± 0.0003	0.0065 ± 0.0009	0.0071 ± 0.0014	0.0048 ± 0.0003	0.0035 ± 0.0014	0.0091 ± 0.0013	0.0056 ± 0.0005	0.0068 ± 0.0011	0.0070 ± 0.0012	0.0078 ± 0.0006
19	Rosiglitazone	0.0226 ± 0.0025	0.0197 ± 0.0005	0.0262 ± 0.0010	0.0379 ± 0.0028	0.0267 ± 0.0012	0.0153 ± 0.0026	0.0262 ± 0.0097	0.0539 ± 0.0068	0.0253 ± 0.0012	0.0505 ± 0.0057	0.0357 ± 0.0067
20	Rosuvastatin	0.1592 ± 0.0183	0.222 ± 0.032	0.2258 ± 0.0231	0.212 ± 0.0171	0.233 ± 0.021	0.122 ± 0.0096	0.126 ± 0.0236	0.189 ± 0.0216	0.138 ± 0.0258	0.145 ± 0.0306	0.183 ± 0.015
21	Saquinavir	0.0064 ± 0.0011	0.0022 ± 0.0003	0.0036 ± 0.0003	0.0038 ± 0.0003	0.0014 ± 0.0002	0.0013 ± 0.0001	0.0015 ± 0.0003	0.0045 ± 0.0004	0.0019 ± 0.0001	0.0039 ± 0.0004	0.0025 ± 0.0002
22	Verapamil	0.0162 ± 0.0017	0.0254 ± 0.0024	0.0202 ± 0.0010	0.0264 ± 0.0024	0.0130 ± 0.0000	0.0162 ± 0.0052	0.0175 ± 0.0013	0.0294 ± 0.0026	0.0123 ± 0.0006	0.0561 ± 0.0054	0.0190 ± 0.0008

Values are the geometric mean ± S.D.

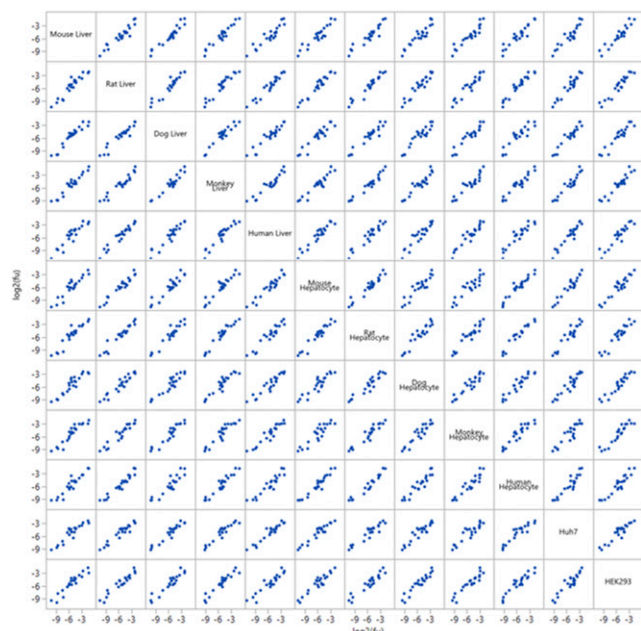


Fig. 2. Pairwise f_u comparisons for various species in liver tissues, hepatocytes, and two cell lines. Sample f_u estimates of 22 compounds across 12 matrices, \log_2 scale, suggests approximate intermatrix agreement.

well. Two hundred microliters of cold ACN with IS was added to precipitate the proteins/tissues. The plates were sealed and mixed with a vortex mixer (VWR) for 1 minute, then centrifuged at 3000 rpm (Beckman Coulter, Fullerton, CA) at room temperature for 5 minutes. The supernatant was transferred to a new 96-deep well plate, dried down, reconstituted, and subsequently analyzed using LC-MS/MS.

LC-MS/MS Analysis. A typical LC-MS/MS method is described here, and equivalent methods were used depending on sample properties. Samples were reconstituted in HPLC grade water/ACN, 50:50 (v/v), vortexed and centrifuged. A 10- μ l aliquot of supernatant was injected onto a LC-MS/MS system using a CTC PAL Autosampler (LEAP Technologies, Morrisville, NC) equipped with a model 1290 binary pump (Agilent, Santa Clara, CA). An ACQUITY UPLC

column (BEH C18, 1.7, 50 \times 2.1 mm; Waters, Milford, MA) was used. A linear HPLC gradient was performed from 95% mobile phase A (0.1% formic acid in water) to 95% mobile phase B (0.1% formic acid in ACN) over 1.1 minutes at a flow rate of 0.5 ml/min to elute the compounds. A triple quadrupole 5500 or 6500 mass spectrometer (Sciex, Foster City, CA) equipped with a turbo ion spray probe and IonDrive Turbo V source was operated in mixed polarity mode. Multiple reaction monitoring was used to detect ion transitions of analytes, along with terfenadine (ESI+) and tolbutamide (ESI-) as ISs. Analyst version 1.6.2 (Applied Biosystems, Foster City, CA) was used for data acquisition, and MultiQuant version 3.0.2 (Applied Biosystems) was applied for quantitation. All calculations were based on area ratios (analyte peak area/IS peak area).

Calculation of f_u , Recovery, and Stability. Diluted f_u ($f_{u,d}$) values of liver tissues and cells were calculated using eq. 1. The area ratios of test compound to IS in receiver and donor wells were determined using LC-MS/MS corrected to account for sampling volume differences. The undiluted f_u of liver tissues and cells was obtained using eq. 2 (Riccardi et al., 2016). Recovery and stability were calculated using eqs. 3 and 4, respectively.

$$\text{Diluted } f_{u,d} = \frac{\text{Receiver Area Ratio}}{\text{Donor Area Ratio}} \quad (1)$$

$$\text{Undiluted } f_u = \frac{1/D}{((1/f_{u,d}) - 1) + 1/D} \quad (2)$$

$$\% \text{ Recovery} = \frac{\text{Donor Area Ratio} + \text{Receiver Area Ratio}}{\text{Donor Area Ratio at Time Zero}} \times 100\% \quad (3)$$

$$\text{Stability as } \% \text{ Remaining} = \frac{\text{Area Ratio at Six Hour}}{\text{Area Ratio at Zero Hour}} \times 100\% \quad (4)$$

Statistical Data Analysis. The f_u quadruplicate distributions were evaluated using standard data analysis methods (Montgomery, 2001) to explore suitable data transformations. Specifically, the log transformation is useful for distributions that are log-normally distributed, subject to proportional errors, have a constant CV, or for variances proportional to the mean squared. To compare the f_u values for the different species and cell types, the log transformation was applied to the geometric mean, a standard summary statistic for skewed assay data, per compound after the quadruplicate evaluation. All statistical inference, excluding standard summary statistics, was performed on the \log_2 scale. The \log_2 scale facilitates comparing f_u ratios per compound across tissues on an additive scale. Pearson correlation coefficient estimates are provided for each pair of species and

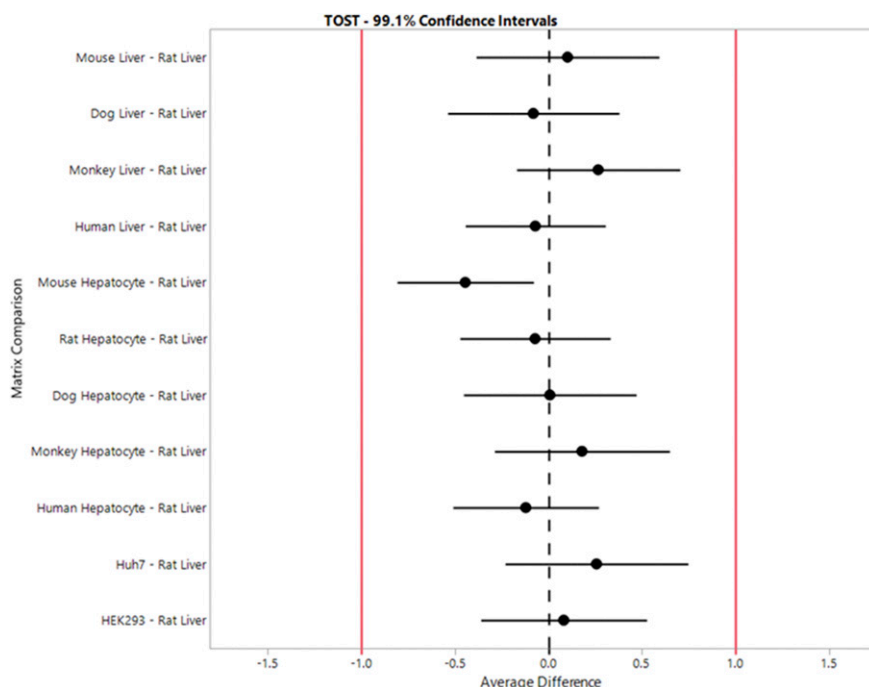


Fig. 3. Average bioequivalence comparison of $f_{u,liver}$ or $f_{u,cell}$. Bonferroni-adjusted CIs for the average f_u matrix difference relative to rat liver f_u on the \log_2 scale for 22 compounds. Average equivalence is declared if the 99.1% CI for the average difference is entirely contained in the ± 1 interval (i.e., within ± 2 -fold on the original scale).

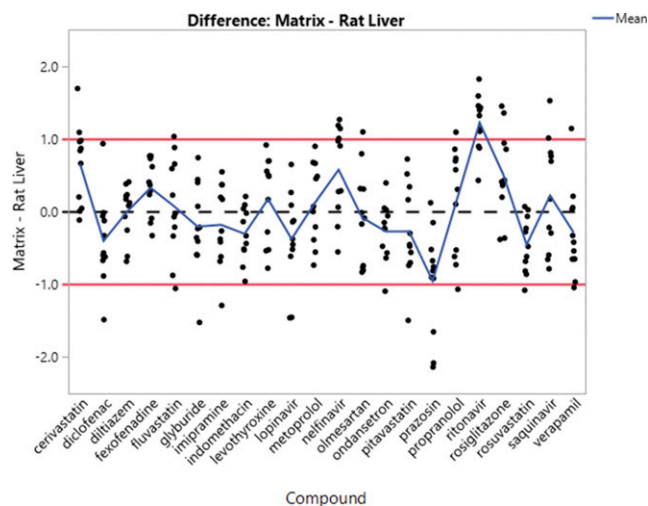


Fig. 4. f_u matrix differences relative to rat liver per compound. f_u values for each matrix minus the corresponding rat liver f_u , \log_2 scale, per compound.

cell-type f_u values. To assess the comparability of the f_u determinations, the two one-sided test (TOST) average bioequivalence procedure outlined in Walker and Nowacki (2011) was used. In standard bioequivalence test settings, the null hypothesis assumes that the average difference between two tissues is larger than a prespecified value; the research hypothesis is that the two tissue averages are equivalent relative to an acceptable difference margin. Here, the margin of equivalence was prespecified at ± 2 -fold [± 1 for a $\log_2(x) - \log_2(y)$ difference and to conveniently aide the data interpretation] from the reference tissue f_u . The rat liver f_u estimate was prespecified as the reference tissue. Normal q-q plots were used to assess the normality of the $\log_2(f_u)$ compound estimates for each tissue. In standard TOST equivalence settings, a 90% confidence interval (CI) for the average difference is computed. Due to the 11 tissue-relative comparisons performed, we applied the Bonferroni correction to retain a family-wise error rate of 0.05. If the adjusted 99.1% CI for an intertissue comparison was contained entirely within the prespecified margin, the two average f_u estimates are declared to be equivalent. JMP version 13.0.0 (SAS Institute, Cary, NC) was used for the statistical analyses.

Results

A set of 22 structurally diverse compounds were used to evaluate the f_u dependency on species and cell type using 12 matrices. The physicochemical properties of the test compounds are shown in Fig. 1. The molecular mass of the compounds ranged from 200 to 800 Da and Log $D_{7.4}$ (lipophilicity) values ranged from -2 to 7 . Acids, bases, neutrals, and zwitterions were included in the test set. The $f_{u,liver}$ values of five species (i.e., mouse, rat, dog, monkey, and human) were determined using equilibrium dialysis method with liver homogenates. In addition, $f_{u,cell}$ values of hepatocytes for five species (mouse, rat, dog, monkey, and human), Huh7 cells, and HEK-293 cells were measured using cell homogenates at cell densities of 40–60 million cells/ml. Huh7 cells were included because it is a hepatocyte-derived cell line with fast growing characteristics and could potentially be used to substitute for expensive hepatocytes in binding studies. Drug transporters (e.g., OATPs, organic anion transporters, and organic cation transporters) are frequently transfected and expressed in HEK-293 cells, and the $f_{u,cell}$ of HEK-293 cells is often measured to obtain intracellular free drug concentration using the binding method (Mateus et al., 2013; Riccardi et al., 2016). Thus, HEK-293 cells were included in the study for comparison purposes. The geometric means of the f_u quadruplicates along with their S.D.s for each matrix are summarized in Table 2. The f_u values range from 0.00052 to 0.51, spanning three \log_{10} units. The average CV for the quadruplicates is 12.5%, suggesting good

TABLE 3
Comparison of $f_{u,cell}$ and $f_{u,inc}$

Characteristics	$f_{u,cell}$	$f_{u,inc}$
Influencing factors	Intrinsic property of a compound	Compound property and incubation conditions
Cell density	Independent of cell density	Decreases with increasing cell density
Measurement	Cell homogenate at high cell density (e.g., 50 million cells/ml)	Cell homogenate at low cell density under incubation conditions (e.g., 0.5–2 million cells/ml)
D	~8 for human hepatocytes at 50 million cells/ml	~800 for human hepatocytes at 0.5 million cells/ml
Definition	Undiluted f_u	Diluted $f_{u,d}$
Values	Generally low, similar to $f_{u,liver}$ for hepatocytes	Generally high, similar to $f_{u,mic}$ with comparable protein level

$f_{u,mic}$, f_u in liver microsomes.

reproducibility of the data across the entire f_u range. This result is similar to previous findings from our laboratory (Riccardi et al., 2015) where it has been demonstrated that the CV does not depend on the magnitude of the f_u (Supplemental Fig. 1) for binding measurements using the equilibrium dialysis assay. This indicates that our f_u determination has comparable precision across the entire f_u range (Riccardi et al., 2015). The f_u comparisons for each pair of matrices for the 22 compounds are plotted in Fig. 2. The correlation coefficients among all the comparisons are close to unity and range from 0.90 to 0.97 (Supplemental Table 1), indicating a strong correlation between f_u determinations per compound across the different species and cell types. These results suggest that one could use a single species/matrix (e.g., rat liver) as a surrogate for $f_{u,liver}$ and $f_{u,cell}$ values of other species. Normal q-q plots of compound-level $\log_2(f_u)$ estimates per matrix suggest that these data are approximately normally distributed (Supplemental Fig. 2). The TOST equivalence test was conducted relative to the rat $f_{u,liver}$ values for each matrix, and the results are shown in Fig. 3. All of the 99.1% adjusted CIs are contained in the ± 1 interval, suggesting average equivalence for each matrix relative to rat $f_{u,liver}$ values for this set of 22 compounds. This suggests that $f_{u,liver}$ and $f_{u,cell}$ values are within an acceptable margin of error across commonly used species and cell types. Based on these results, we propose that rat $f_{u,liver}$ be used as a surrogate for determinations of $f_{u,liver}$ and $f_{u,cell}$ values for other species and cell types in drug discovery. The differences between rat $f_{u,liver}$ and the other matrices were also examined for compound dependencies. Despite the intrinsic experimental uncertainty of the rat $f_{u,liver}$ estimate, the other f_u matrix estimates for a given compound were generally within ± 2 -fold (Fig. 4). Across all of the 22 compounds tested, only one compound, ritonavir, resulted in an average f_u difference greater than 2-fold. This suggests that under the current equilibrium dialysis method, rat liver serves as a suitable matrix for f_u assessments that could be adapted for most drug discovery compounds.

Discussion

This study of a diverse set of 22 compounds and with a wide range of f_u values in 12 different matrices showed that $f_{u,liver}$ and $f_{u,cell}$ values were independent of the species and cell types commonly used in drug discovery. To the best of our knowledge, this is the first study comparing species differences in the binding of liver tissues, hepatocytes, and other cell types. We propose that rat $f_{u,liver}$ be used as a surrogate for $f_{u,liver}$ and $f_{u,cell}$ for other species and cell types. This offers the potential to greatly simplify binding studies to enable effective determination of free liver drug concentrations in multiple species, intracellular free drug concentrations in cell-based assays, and in vitro and in vivo K_{puu} . Our

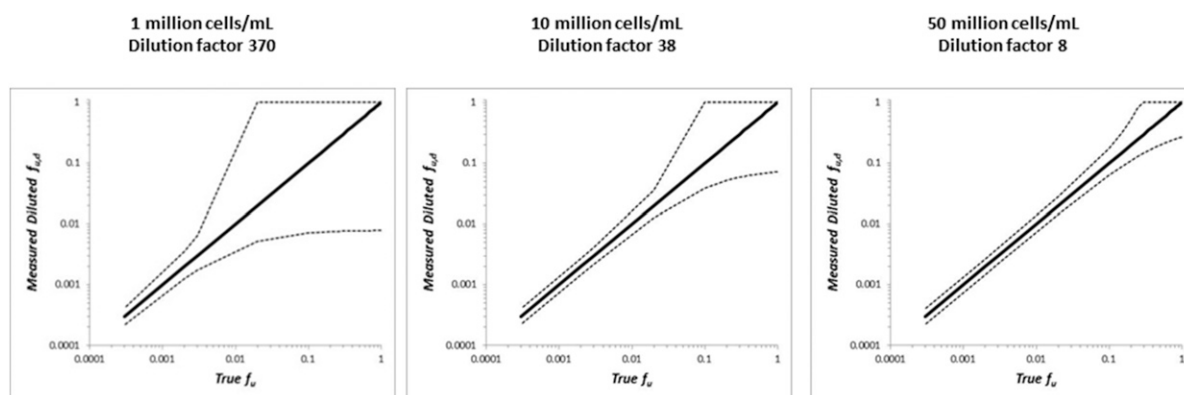


Fig. 5. Effect of cell density and D on undiluted f_u . Assume that the human hepatocyte diameter is $17.3 \mu\text{m}$ and the CV for $f_{u,d}$ measurement is 15%. Dotted lines represent 95% CI. f_u values that can be accurately measured decreased with increased D or decreased in cell density.

findings are consistent with studies reported previously that binding to liver microsomes is mostly driven by nonspecific binding to phospholipids, which is species independent (Margolis and Obach, 2003). The results are also in good agreement with the observation that f_u values of hepatocytes correlate well with those from HEK-293 cells (Mateus et al., 2013). Hepatocytes account for approximately 80% of the liver volume (Kmiec, 2001); therefore, the binding to liver tissue is expected to be similar to that of hepatocytes. Both $f_{u,liver}$ and $f_{u,cell}$ are mainly driven by nonspecific binding to phospholipids from cell membranes and liver tissues.

Plasma protein binding can be measured by using plasma directly without the need of any dilution. In contrast, tissues cannot be used directly for binding studies, and they are usually diluted with buffer and homogenized prior to binding experiments. Therefore, the $f_{u,d}$ is measured directly from experiments, and the undiluted f_u values are derived using eq. 2. For cell-binding ($f_{u,cell}$) measurements, it is slightly more complicated because it is often confused with fraction unbound under incubation conditions ($f_{u,inc}$) in cell-based assays (binding under incubation conditions with hepatocytes for metabolic stability or other experiments). The comparison of $f_{u,cell}$ and $f_{u,inc}$ is shown in Table 3. $f_{u,cell}$ is a measure of nonspecific binding of a compound in cell homogenates. It is considered to be an intrinsic property of a compound and is independent of cell density in the incubation when sufficient cells are used for measurement. $f_{u,inc}$, on the other hand, is dependent on the properties and cell density of a compound in the incubation. The higher the cell density, the lower the $f_{u,inc}$ value. $f_{u,cell}$ is typically measured by using cell homogenates at high cell density (e.g., 50 million cells/mL; see Discussion below on the limitations of using a low cell density), and the value is usually much lower than that for $f_{u,inc}$ but is similar to that for $f_{u,liver}$. $f_{u,cell}$

can also be measured with whole cells at 4°C with the correction of the pH-gradient effect (i.e., $f_{u,cell} = 1/\text{partition coefficient at } 4^\circ\text{C}$), where active processes by transporters and enzymes and membrane potentials are essentially shut down at low temperature (Dipolo and Latorre, 1972; Fischbarg, 1972). The $f_{u,inc}$, on the contrary, is usually determined using cell homogenates or dead cells at lower cell densities, the same as under the incubation conditions for metabolic stability studies (e.g., 0.5–2 million cells/mL). $f_{u,inc}$ values are typically much higher than $f_{u,cell}$ values, but values are similar to those for f_u in liver microsomes at a comparable protein concentration. Since both $f_{u,cell}$ and $f_{u,inc}$ use cell homogenates for measuring binding, they are sometimes confused as being the same. $f_{u,cell}$ is an undiluted f_u and needs to be corrected once measured from diluted cell homogenates based on a D calculated from cell density and cell diameter (eq. 2). $f_{u,inc}$ is an $f_{u,d}$, and it is measured directly from cell homogenates using incubation cell density and calculated using eq. 1. No D correction is needed for $f_{u,inc}$. The relationship between $f_{u,cell}$ (undiluted f_u) and $f_{u,inc}$ ($f_{u,d}$) can be described by eq. 2 only when cell density is high enough (i.e., low D), especially for weakly bound compounds.

The impact of cell density and D on undiluted f_u is shown in Fig. 5 and Table 4. When the cell density is too low (D is too high), $f_{u,d}$ is too high for compounds that are not highly bound, and the variability can be very large when converted back to the undiluted f_u value. Therefore, in practice, to be able to accurately determine $f_{u,cell}$ values, the measured $f_{u,d}$ value needs to be sufficiently low by selecting the appropriate cell density or D for tissue homogenates. This means that for highly bound compounds the cell density can be lower (e.g., 20 million cells/mL); but, for weakly bound compounds the cell density needs to be higher (e.g., 50 million cells/mL) to ensure an accurate conversion back to the undiluted $f_{u,cell}$. Cell density (or D) is important for measuring $f_{u,cell}$. The observed differences in $f_{u,cell}$

TABLE 4
Effects of cell density and D on undiluted f_u

Cell Density million cells/mL	D	0.01	0.05	0.1	0.3	0.5	0.7	0.9	0.99	True f_u
1	370	0.79	0.95	0.98	0.99	1.00	1.00	1.00	1.00	Measured $f_{u,d}$
2	186	0.65	0.91	0.95	0.99	0.99	1.00	1.00	1.00	
5	75	0.43	0.80	0.89	0.97	0.99	0.99	1.00	1.00	
10	38	0.28	0.67	0.81	0.94	0.97	0.99	1.00	1.00	
20	19	0.16	0.50	0.68	0.89	0.95	0.98	0.99	1.00	
50	8	0.07	0.30	0.47	0.77	0.89	0.95	0.99	1.00	
100	5	0.05	0.21	0.36	0.68	0.83	0.92	0.98	1.00	
200	3	0.03	0.14	0.25	0.56	0.75	0.88	0.96	1.00	
1000	1	0.01	0.05	0.10	0.30	0.50	0.70	0.90	0.99	

Assume that the cell diameter is $17.3 \mu\text{m}$.

between hepatocytes and HEK-293 cells in the previous study might be due to too high a D caused by a low cell density (Mateus et al., 2013). The cell density for measuring $f_{u,inc}$ under hepatocyte stability conditions is usually too low to generate reliable $f_{u,cell}$ values, although they are perfectly fine to be used to correct for unbound intrinsic clearance. This study also suggests that a single-species microsomal or hepatocyte binding (e.g., $f_{u,inc}$ for rat) can be used as a surrogate for $f_{u,inc}$ for all species with adjustment for protein concentration, when correcting for unbound concentration in *in vitro* incubations.

This species and cell-type comparison study in liver tissue, hepatocytes, and two cell lines (Huh7 and HEK-293) showed that $f_{u,liver}$ is species independent and is comparable with $f_{u,cell}$ from different cell types. $f_{u,liver}$ from a single species (e.g., rat) can be used as a surrogate for liver binding of other species as well as $f_{u,cell}$ of various cell types. $f_{u,cell}$ should not be confused with $f_{u,inc}$ in hepatocytes. They are very different and are used for different applications. This study also suggests that $f_{u,inc}$ with a single species (e.g., rat) can be used to replace $f_{u,inc}$ for other species.

Acknowledgments

We thank Karen Atkinson for her help with database search efforts and Patrick Trapa for useful discussion.

Authorship Contributions

Participated in research design: Riccardi, Ryu, Lin, Yates, Tess, Li, Singh, Holder, Kapinos, Chang, and Di.

Conducted experiments: Riccardi, Ryu, Lin, Singh, Holder, and Kapinos.

Performed data analysis: Riccardi, Ryu, Lin, Yates, Tess, Singh, Holder, Kapinos, Chang, and Di.

Wrote or contributed to the writing of the manuscript: Riccardi, Ryu, Lin, Yates, Li, Holder, Chang, and Di.

References

- Di L and Kerns EH (2016) *Drug-Like Properties: Concepts, Structure Design, and Methods*, Elsevier, London.
- Di L, Umland JP, Chang G, Huang Y, Lin Z, Scott DO, Troutman MD, and Liston TE (2011) Species independence in brain tissue binding using brain homogenates. *Drug Metab Dispos* **39**:1270–1277.
- Dipolo R and Latorre R (1972) Effect of temperature on membrane potential and ionic fluxes in intact and dialysed barnacle muscle fibres. *J Physiol* **225**:255–273.
- Fischbarg J (1972) Ionic permeability changes as the basis of the thermal dependence of the resting potential in barnacle muscle fibres. *J Physiol* **224**:149–171.

- Kmieć Z (2001) Cooperation of liver cells in health and disease. *Adv Anat Embryol Cell Biol* **161**:III–XIII, 1–151.
- Kratohvil NA, Huber W, Müller F, Kansy M, and Gerber PR (2004) Predicting plasma protein binding of drugs—revisited. *Curr Opin Drug Discov Devel* **7**:507–512.
- Li R, Barton HA, Yates PD, Ghosh A, Wolford AC, Riccardi KA, and Maurer TS (2014) A “middle-out” approach to human pharmacokinetic predictions for OATP substrates using physiologically-based pharmacokinetic modeling. *J Pharmacokinet Pharmacodyn* **41**:197–209.
- Margolis JM and Obach RS (2003) Impact of nonspecific binding to microsomes and phospholipid on the inhibition of cytochrome P4502D6: implications for relating *in vitro* inhibition data to *in vivo* drug interactions. *Drug Metab Dispos* **31**:606–611.
- Mateus A, Gordon LJ, Wayne GJ, Almqvist H, Axelsson H, Seashore-Ludlow B, Treyer A, Matsson P, Lundbäck T, West A, et al. (2017) Prediction of intracellular exposure bridges the gap between target- and cell-based drug discovery. *Proc Natl Acad Sci USA* **114**:E6231–E6239.
- Mateus A, Matsson P, and Artursson P (2013) Rapid measurement of intracellular unbound drug concentrations. *Mol Pharm* **10**:2467–2478.
- Montgomery D (2001) *Design and Analysis of Experiments*, John Wiley & Sons, Inc., New York.
- Oballa RM, Belair L, Black WC, Bleasby K, Chan CC, Desroches C, Du X, Gordon R, Guay J, Guiral S, et al. (2011) Development of a liver-targeted stearyl-CoA desaturase (SCD) inhibitor (MK-8245) to establish a therapeutic window for the treatment of diabetes and dyslipidemia. *J Med Chem* **54**:5082–5096.
- Pfefferkorn JA (2013) Strategies for the design of hepatoselective glucokinase activators to treat type 2 diabetes. *Expert Opin Drug Discov* **8**:319–330.
- Pfefferkorn JA, Guzman-Perez A, Litchfield J, Aiello R, Treadway JL, Pettersen J, Minich ML, Filipinski KJ, Jones CS, Tu M, et al. (2012) Discovery of (S)-6-(3-cyclopentyl-2-(4-(trifluoromethyl)-1H-imidazol-1-yl)propanamido)nicotinic acid as a hepatoselective glucokinase activator clinical candidate for treating type 2 diabetes mellitus. *J Med Chem* **55**:1318–1333.
- Read KD and Braggio S (2010) Assessing brain free fraction in early drug discovery. *Expert Opin Drug Metab Toxicol* **6**:337–344.
- Riccardi K, Cawley S, Yates PD, Chang C, Funk C, Niosi M, Lin J, and Di L (2015) Plasma protein binding of challenging compounds. *J Pharm Sci* **104**:2627–2636.
- Riccardi K, Li Z, Brown JA, Gorgoglione MF, Niosi M, Gosset J, Huard K, Erion DM, and Di L (2016) Determination of unbound partition coefficient and *in vitro-in vivo* extrapolation for SLC13A transporter-mediated uptake. *Drug Metab Dispos* **44**:1633–1642.
- Riccardi K, Lin J, Li Z, Niosi M, Ryu S, Hua W, Atkinson K, Kosa RE, Litchfield J, and Di L (2017) Novel method to predict *in vivo* liver-to-plasma K_{puu} for OATP substrates using suspension hepatocytes. *Drug Metab Dispos* **45**:576–580.
- Riede J, Poller B, Huwyler J, and Camenisch G (2017) Assessing the risk of drug-induced cholestasis using unbound intrahepatic concentrations. *Drug Metab Dispos* **45**:523–531.
- Smith DA, Di L, and Kerns EH (2010) The effect of plasma protein binding on *in vivo* efficacy: misconceptions in drug discovery. *Nat Rev Drug Discov* **9**:929–939.
- Summerfield SG, Lucas AJ, Porter RA, Jeffrey P, Gunn RN, Read KR, Stevens AJ, Metcalf AC, Osuna MC, Kilford PJ, et al. (2008) Toward an improved prediction of human *in vivo* brain penetration. *Xenobiotica* **38**:1518–1535.
- Sun Y, Chothe PP, Sager JE, Tsao H, Moore A, Laitinen L, and Hariparsad N (2017) Quantitative prediction of CYP3A4 induction: impact of measured, free, and intracellular perpetrator concentrations from human hepatocyte induction studies on drug-drug interaction predictions. *Drug Metab Dispos* **45**:692–705.
- Tu M, Mathiowetz AM, Pfefferkorn JA, Cameron KO, Dow RL, Litchfield J, Di L, Feng B, and Liras S (2013) Medicinal chemistry design principles for liver targeting through OATP transporters. *Curr Top Med Chem* **13**:857–866.
- Walker E and Nowacki AS (2011) Understanding equivalence and noninferiority testing. *J Gen Intern Med* **26**:192–196.

Address correspondence to: Li Di, Pharmacokinetics, Dynamics and Metabolism, Pfizer Inc., Eastern Point Road, Groton, CT 06340. E-mail: li.di@pfizer.com